IEEE Access
Multidisciplinary | Rapid Review | Open Access Journal

Date of publication xxxx 00, 0000, date of current version xxxx 00, 0000.

Digital Object Identifier 10.1109/ACCESS.2017.Doi Number

Wavelet-Multi Resolution Analysis Based ANN Architecture for Fault Detection and Localization in DC Microgrids

D.K.J.S Jayamaha [1], Graduate Student Member, IEEE, N.W.A Lidula [1], Member, IEEE and A.D Rajapakse[2], Senior Member, IEEE

[1]Department of Electrical Engineering, University of Moratuwa, Katubedda, Moratuwa, Sri Lanka
[2]Department of Electrical and Computer Engineering, University of Manitoba, MB, R3T 5V6, Canada

Corresponding author: D.K.J.S Jayamaha (e-mail: shanjayamah@gmail.com).

This work was supported by the University of Moratuwa, Sri Lanka under the research grant SRC/CAP/2018/1

ABSTRACT DC microgrids present an effective power system solution for increased integration of renewable sources while providing clear benefits, such as high efficiency and simpler control. However, the protection of DC networks still remains a challenge due to strict time limits for fault interruption imposed by fast rising fault currents in DC systems, and absence of frequency and phasor information. This paper introduces a technique for fast detection and isolation of the faults in the DC microgrids without de-energizing the whole network. In the proposed algorithm, branch current measurements are sampled and Wavelet transform is applied to capture the characteristic changes in the current signals caused by network faults. The temporal variations in the relative wavelet energy within the frequency bands are acquired to construct the feature vector for classification. Artificial neural networks are used as the classifier as it provides a soft criterion for fault detection, featuring smart fault detection capability. The relatively fast calculation time of artificial neural networks makes it a good candidate for this application, due to the strict time restrictions inherited in DC fault isolation. To evaluate the performance, a comprehensive study on the proposed scheme is presented. The results demonstrate the effectiveness of the proposed scheme in terms of fast and reliable fault detection and inbuilt accurate fault localization capability.

INDEX TERMS Artificial Neural Networks, DC microgrid protection, Fault detection, Fault localization, Wavelet transform

I. INTRODUCTION

DC microgrids (DCMGs) have the potential to offer more efficient integration of distributed generators (DGs) such as solar PVs and battery energy storages, and electronic loads, due to the reduced power conversion stages. With the new developments in the power sector, smart homes/ buildings, vehicle to grid technology, hybrid energy storages, and renewable energy parks, DCMGs have immerged as an interesting option for future power systems. However, the absence of effective solutions for fault detection in DC distribution systems represents a significant barrier for widespread adoption of DCMGs [1, 2].

The inherent absence of frequency and phasor information in DC systems prevents the direct adoption of line impedance based methods, as in AC systems. Hence, overcurrent, rate of current rise and differential elements are commonly used for DC network protection [3-5]. However, due to the intermittent nature of DGs connected to the DCMGs, different operational modes and high sensitivity of the network response to the fault impedance, protection of DCMGs is challenging [4-7]. Furthermore, changing fault level, changing power flow direction and complex network architectures may lead to suboptimal fault discrimination; hence, poses a challenge in relay coordination [3, 4].

Fault localizing is a crucial requirement as quick isolation of the faulty section of the network is essential to enable fast recovery of the network [5-7]. To achieve a greater level of selectivity and fault localizing capability, implementations of communication-based unit protection schemes are discussed in the literature [3-6]. However, the scope for the implementation of such schemes is typically limited due to the additional cost of the necessary communication. Furthermore, dependency on multi-

This article has been accepted for publication in a future issue of this journal, but has not been fully edited. Content may change prior to final publication. Citation information: DOI 10.1109/ACCESS.2019.2945397, IEEE Access

terminal measurements, accuracy affected by communication delays and sensor errors, and the requirement for synchronized measurements prevent the widespread adoption of communication-based schemes.

DC microgrids mostly comprise of power electronic converters for interfacing DGs and loads to the DC bus. Power electronic components have limited overcurrent withstand capability, typically in the range of 2-3 times nominal load current for a few tens of milliseconds [8]. In addition, DC networks have very short time constants, resulting in a rapid rise in fault current during a fault, particularly due to the DC bus capacitor discharge [7, 8]. Consequently, a fault in a DC network should be detected and isolated before reaching critical fault current levels [3, 7, 8].

While there are solid-state circuit breaker and hybrid circuit breaker technologies, which can meet the strict time limits for fault interruption in DC networks, a reliable technique for fast detection and isolation of DC network faults without de-energizing the whole network, is a crucial requirement [8-10].

Recently, a growing body of research adopts digital signal processing and data-driven techniques for power system event recognition [11-13]. Digital signal processing based techniques such as short-time Fourier transform and wavelet transform (WT) are among widely adopted methods used for frequency and time-domain analysis. Short-time Fourier transform based fault detection scheme for a VSC interfaced DC distribution network is presented in [14]. Short-time Fourier transform has its drawbacks such as limited time-frequency resolution. Low frequencies can be hardly depicted with short windows, whereas high frequencies can only be poorly localized in time with a long data window [11]. Conversely, WT has the ability to decompose a signal into specific time-frequency resolutions. Hence, it can better capture the abrupt changes of a signal caused by a fault in a power network. Wavelet transform based techniques have been proposed extensively for several power system applications, including fault classification and network event recognition [11-13]. In [15] percentage change in decomposition level energy is compared for fault detection in DCMGs. Wavelet transform is applied to decompose common mode current measured at different network points, to detect and locate ground faults in DCMGs in [16].

Digital signal processing techniques such as WT is prone to noise and network disturbances. Machine learning models using a soft criterion for fault detection as opposed to hard thresholds endows robustness against measurement uncertainty to the fault detection scheme. Models such as decision trees, artificial neural networks (ANNs), support vector machines, deep neural networks, and K-nearest neighbor has been employed in power system fault detection in literature [17-22]. Good generalization capability along with the high computational speed of machine learning algorithms offer intelligent and fast fault detection capability, unaffected by noise and disturbances in the network. An investigation into the use of machine learning models including ANNs, decision trees and support vector machines for fault detection in DC shipboard networks is presented in [23]. Application of ANNs for detection of classification of faults according to fault type and location in DCMG networks are presented in [24, 25]. These proposed schemes directly use sampled current measurements for training and classifying fault events, leading to complex ANN structures, and longer detection times.

However, there remains a research gap for the formulation of accurate fault detection and localization scheme for DCMGs. Most of the existing techniques utilizing signal processing and data-driven technique for fault detection and localization focuses on AC distribution networks [19-21]. Currently, most of the DCMG protection techniques rely on communication between devices, which results in several practical issues in implementation. Moreover, the existing signal processing and data-driven techniques for DCMG protection require further improvements to address issues; absence of fault localization and selective isolation capability, vulnerability to noise, and complex algorithms leading to longer fault detection time.

To address the research gap of fault detection and localization in DCMGs, in this paper, an intelligent scheme based on WT and ANN is proposed. Compared to existing DCMG fault detection schemes, the proposed scheme is capable of providing fast and accurate fault detection results, facilitating quick isolation of the faulted segment of the network. The proposed method does not require communication infrastructure and eliminates the requirement for synchronized measurements. Furthermore, it offers intelligent fault detection capability under different operating modes, loading conditions, and has the capability to differentiate non-fault power dynamics from fault conditions.

The rest of the paper is organized as follows: Section II describes the notional DCMG model used to analyze the proposed scheme. Fault detection and localization requirements are identified, and relay coordination strategy is proposed in section III. The general structure of the proposed fault detection and localization algorithm is introduced in section IV. Section V presents the wavelet theory, fault feature extraction and variations in selected feature vector with different network events. Structure of the adopted ANNs is discussed in Section VI. Section VII summarizes the test results and analyzes the performance of the proposed fault detection scheme. Finally, section VIII draws the conclusions.

II. THE DC MICROGRID

To verify the fault detection and localization scheme proposed in this paper, notional DCMG modeled in PSCAD/EMTDC is employed. Simplified schematic of the

This article has been accepted for publication in a future issue of this journal, but has not been fully edited. Content may change prior to final publication. Citation information: DOI 10.1109/ACCESS.2019.2945397, IEEE Access

model is shown in Fig. 1. The DCMG operates in either grid-connected or islanded mode. Battery storage system and a photovoltaic power source are interfaced to the DC bus through Power electronic converters [26].

Digital protective relays along with fast-acting DC circuit breakers are deployed in the network on selected strategic locations to implement a coordinated fault detection and interruption scheme. These relays sample branch current measurements at 50 kHz rate and are then pre-processed for fault detection and localization.

III. PROTECTION COORDINATION REQUIREMENTS

An effective protection coordination strategy minimizes the critical fault clearing time, enables quick system restoration and fault ride-through capability, and minimizes outages; thereby, it ensures the reliability and safety of the network [27]. Protection coordination issues bring many challenges; selection of protection equipment to optimize the fault clearing with minimum outages, and miscoordination between devices are among these [4, 27].

This Section presents a protection coordination strategy to be deployed with the proposed fault detection and localization scheme. As shown in Fig. 1, the network is segmented into several zones by selective positioning of DC circuit breakers, and these breakers in conjunction with digital relays operate to isolate the fault zone, in the event of a fault. Backup protection is also implemented for the relevant relays and circuit breaker failures to improve system reliability.

The proposed fault detection algorithm can be implemented and executed by digital relays monitoring the branch current signals at each branch node, as in Fig. 1. Table I presents the proposed coordination strategy between relays, to provide primary and backup protection to different components of the network from pole-ground and pole-pole faults, occurring at different locations of the network. For the faults occurring at load feeders, it is important to isolate the faulted load feeder to protect the other components in the network. Relays R_4, R_5, R_6 and R_7 provide primary protection against faults occurring in each load feeders (zones 2, 3, 4 and 5). The primary protection zones of the DCMG model are shown in Fig. 1. For the faults occurring at the zone 1 (see Fig. 1), relays R_1, R_2, and R_3 picks up the fault (primary protection), and fault current contribution from the utility grid, solar PV and battery storage is cutoff by DC circuit breakers. Relays R_1, R_2, and R_3 provide backup protection against faults occurring in the zones 2, 3, 4 and 5, in case of breaker or relay failures at the load feeders, and is shown in Fig. 1.

The proposed protection coordination strategy is implemented using two types of time graded relays, rendering selectivity in fault interruption, and is discussed in later Sections.

IV. PROPOSED FAULT DETECTION AND LOCALIZATION SCHEME

The flowchart of the proposing fault detection algorithm is shown in Fig. 2. Sampled current measurements at digital relays are pre-processed by discrete wavelet transform (DWT) to extract the "fault features" in both time and frequency domain. The extracted feature vector is fed into the ANN for fault detection and classification. Time series variation of relative wavelet energy (RWE) in each DWT decomposition level is acquired embedding time-series data to construct the feature vector, and is discussed below. DWT based signal decomposition and the use of ANN for fault detection and event classification will be further discussed in sections V and VI.

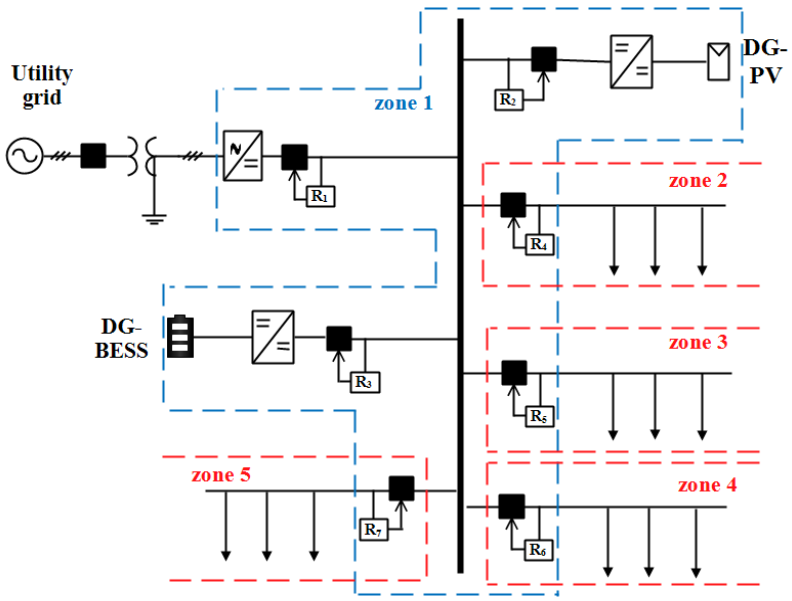

FIGURE 1: Schematic of the notional DC microgrid model and the protection zones

This article has been accepted for publication in a future issue of this journal, but has not been fully edited. Content may change prior to final publication. Citation information: DOI 10.1109/ACCESS.2019.2945397, IEEE Access

TABLE I
DCMG FAULT LOCATIONS AND CORRESPONDING PROTECTION DEVICES SELECTED FOR THE PROTECTION OF DCMG COMPONENTS.

DCMG Component	Primary protection		Backup protection	
	Dc bus faults	Lateral feeder fault	DC bus fault	Lateral feeder fault
Power converter protection	DC circuit breakers and Relays R_1, R_2 and R_3	DC circuit breakers, and relays R_4, R_5, R_6 and R_7	None	DC circuit breakers and relays R_1, R_2 and R_3
Battery protection	DC circuit breakers and relay R_3	DC circuit breakers and relays at R_4, R_5, R_6 and R_7	None	DC circuit breakers and relay R_3
Solar PV protection	DC circuit breakers and relay R_2	DC circuit breakers and relays R_4, R_5, R_6 and R_7	None	DC circuit breakers and relay R_2
Load Feeder protection	None	DC circuit breaker and relays R_4,R_5, R_6 and R_7	None	DC circuit breakers and relays R_1,R_2 and R_3

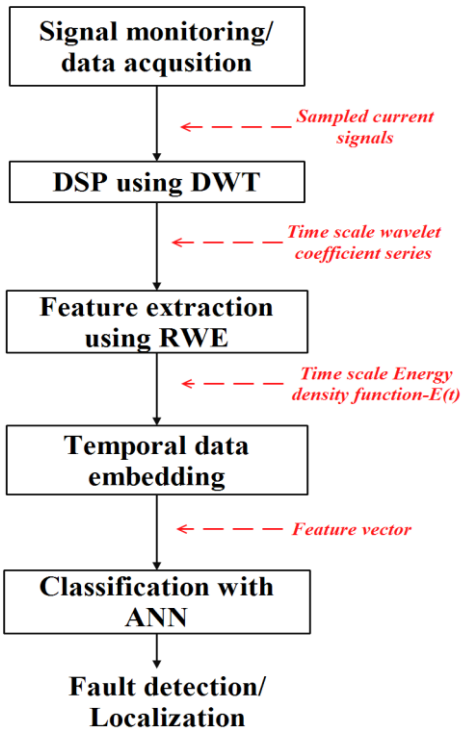

FIGURE 2: Flowchart of the proposed fault detection algorithm

A. EMBEDDING TEMPORAL DATA TO CONSTRUCT THE FEATURE VECTOR

Most of the classifier models including ANN overlook the temporal dependencies of the input data. The data correlation in the time domain is crucial in identifying the network events, as most of them are dynamic in nature [28].

In the proposed scheme, a shift register of delays are employed, where successive data of the time series can be retained. This allows the time-series data to be used as a spatial vector, to input into a classifier, enabling accurate classification, as the ANN can capture the temporal dependencies within the data window considered. Implicit transformation of time series data into a spatial vector is called embedding, and is a widely recognized technique used to classify and predict events using temporal data [29, 30].

As shown in Fig. 3, at each instant ***t***, we can truncate the time series data to only the previous ***d*** number of samples to formulate the feature vector for the classifier. Here, ***d*** is called embedding dimension [30, 31].

B. SELECTION OF RELAYS FOR PROPER COORDINATION

This paper proposes a relay coordination scheme for fault localization and isolation, implemented by time grading of the relays. To maintain proper coordination, load feeder primary protection relays R_4, R_5, R_6 and R_7 are required to operate prior to relays R_1, R_2 and R_3. Hence, the relays are time graded such that relays R_4, R_5, R_6 and R_7 operates prior to the relays R_1, R_2 and R_3. This time grading also allows the relays R_1, R_2 and R_3 to back up the relays R_4, R_5, R_6 and R_7. Accordingly, two types (*type I* and *type II*) of time graded relays are employed. Two different ***d*** values are used in embedding time-series data into two spatial vectors of different dimensions. To fulfill the protection coordination requirements discussed in Section III, the relays are selected as given in Table II.

Embedding dimension, ***d*** was selected on the basis of fault detection accuracy and ability to maintain proper coordination between two types of relays. The initial studies showed that the classification accuracies improve with increasing values of ***d***. However, increasing values of ***d*** mean longer embedding time delay, resulting in longer fault detection time. This tradeoff between classification accuracy and speed of detection must be considered in selection of ***d***. In this study we employ ***d***= 2 for *type I* relays. In order to allow proper time discrimination between upstream and downstream relays, ***d***= 4 is selected for *type II* relays. This allows *type II* relays to identify fault interruption operations by primary protection relays (*type I* relays) of zones 2, 3, 4 and 5 (lateral load feeders).

This article has been accepted for publication in a future issue of this journal, but has not been fully edited. Content may change prior to final publication. Citation information: DOI 10.1109/ACCESS.2019.2945397, IEEE Access

TABLE II
RELAY TYPE SELECTION AND PROTECTED ZONES OF THE DCMG NETWORK

Relay	Relay type	Protected zone of the DCMG
R_1	*Type II*	Primary protection – zone 1 Backup for- zones 2,3,4 and 5
R_2	*Type II*	Primary protection – zone 1 Backup for- zones 2,3,4 and 5
R_3	*Type II*	Primary protection – zone 1 Backup for- zones 2,3,4 and 5
R_4	*Type I*	Primary protection – zone 2
R_5	*Type I*	Primary protection – zone 3
R_6	*Type I*	Primary protection – zone 4
R_7	*Type I*	Primary protection – zone 5

V. WAVELET ANALYSIS AND FEATURE EXTRACTION

Wavelet Transform (WT) is a signal processing technique frequently used for applications in power system studies [11-13, 32, 33]. The WT decompose wideband and non-stationary signals into specific time-frequency resolutions. The ability of the WT to localize a signal in both time and frequency domains makes it possible to capture the abrupt changes of signals and localize their occurrence [32-35].

In the proposed fault detection and classification scheme, a variant of WT, discrete wavelet transform (DWT) serves an important element in extracting the fault features. A brief introduction into the wavelet theory, and DWT based multi-resolution analysis is given in the appendix.

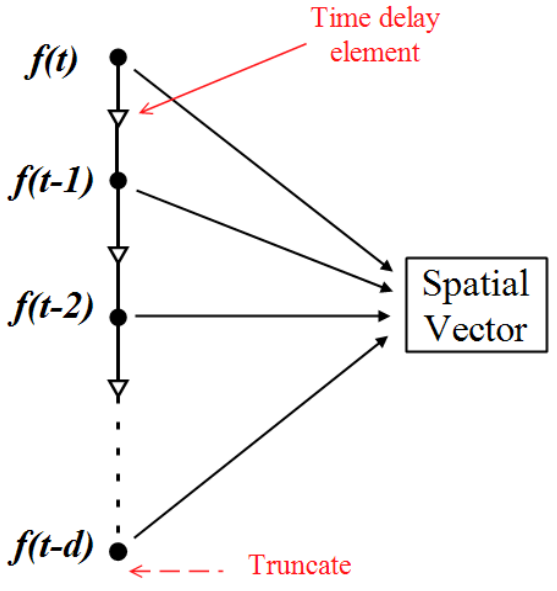

FIGURE 3: Technique for embedding temporal data to construct a spatial vector

A. MOTHER WAVELET AND DECOMPOSITION LEVEL SELECTION

In WT analysis there are many wavelet families (eg: - Daubechies family (dbN), Symlets family (symN) and Coiflets family (coifN)), which can be used as mother wavelet. Where, N is the order of the wavelet function. Generally, mother wavelets are characterized by properties such as orthogonality, compact support, symmetry and vanishing moments. These properties are considered in selecting a mother wavelet [36]. In general, db wavelets compared to other wavelets provide good signal recognition and noise removal capabilities. When analyzing power network signals which usually contains large amount of transient components, db wavelets are deemed suitable as the mother wavelet [16]. Hence, db wavelet family is chosen for analysis, in this study.

With db as the base function, db1-db10 are the most commonly used among dbN series wavelet. In this study, the selection of dbN series wavelet is based on accuracy of the classifier scheme resulting from each series wavelet concerned. The initial studies with wavelets db1-db10 using a trial and error approach showed that db5 wavelet renders the best classification accuracies for this application. Accordingly, db5 mother wavelet was selected as it will provide optimal fault detection and localization performance.

Decomposition level is another parameter that affects the signal feature extraction process. Decomposition level is selected to capture all the high-frequency content contained in the signal that is necessary for feature comparison. However, higher decomposition level will result in longer temporal window for RWE calculation, which in turn results in longer classification time [34]. Consequently, the current signal is decomposed into 6 levels of decomposition for feature extraction. With the sampling frequency of 50 kHz, frequency bands of the high-frequency components captured by each decomposition level are shown in Table III.

TABLE III
FREQUENCY BANDS OF DWT DECOMPOSITION LEVELS, AND MINIMUM WINDOW SIZE FOR RWE CALCULATION IN EACH DECOMPOSITION LEVEL

DWT decomposition level	Frequency bands (Hz)	Minimum window size for RWE calculation
1	25 k - 12.5 k	0.04 ms
2	12.5 k - 6.25 k	0.08 ms
3	6.25 k - 3.125 k	0.16 ms
4	3.125 k -1.5625 k	0.32 ms
5	1565.5 - 781.25	0.64 ms
6	781.25 - 390.62	1.28 ms

This article has been accepted for publication in a future issue of this journal, but has not been fully edited. Content may change prior to final publication. Citation information: DOI 10.1109/ACCESS.2019.2945397, IEEE Access

B. FAULT FEATURE EXTRACTION

The wavelet detail coefficients provide a portrayal of the energy distribution of the monitored current signal, in different frequency bands. Using these coefficients directly, as a learning parameter of a classifier requires large memory space and processing time. Furthermore, classification accuracy resulting from using the detail coefficients is very poor. Hence, the selection of an information tool with reduced quantities, but without losing the properties of the original signal is a crucial requirement for the performance of the classifier [12, 13]. In the proposed scheme RWE of the detail coefficients is selected as a tool to construct the input feature vector for ANN.

1) RELATIVE WAVELET ENERGY

The concept of wavelet energy is linked to the usual notions derived from Fourier theory [37, 38]. The energy content of the detail coefficients of a decomposition level can be defined for a selected temporal window as in (1),

$$E_j = \sum_K |d_j(K)|^2 \qquad (1)$$

Where, j is the decomposition level, K is the discrete time location, d_j is the wavelet coefficients and E_j wavelet energy of the j^{th} decomposition level. Hence, a sliding window can capture the trend of variation of wavelet energy of a signal at each decomposition level [37].

The total wavelet energy, E_{Tot} of all the decomposition levels can be obtained using (2),

$$E_{Tot} = \sum_j \sum_K |d_j(K)|^2 \qquad (2)$$

The RWE, given by (3) yields the probability distribution for the wavelet energy at different decomposition levels $j=1,2,....n$.

$$RWE_j = E_j / E_{Tot} \qquad (3)$$

Variation of RWE_j in time can be considered a time scale probability density function. The RWE has demonstrated its effectiveness in the previous studies for detecting and classifying specific events in both time and frequency scales [20, 38, 39].

In this study, in order to follow the temporal variations of RWE, wavelet coefficient series $\{d_{j,k}\}$, is divided into non-overlapping temporal windows of equal length.

2) FEATURE EXTRACTION RESULTS

To verify the proposed approach, using DWT based Multi-resolution analysis, and RWE as the information tool, feature vectors under different faults and non-fault events are extracted. Signals under analysis are decomposed into six detail levels and RWE of each level is calculated.

To improve the time resolution of the proposed scheme, it is important that we select the smallest possible time window for RWE calculation. There is a limit to the time resolution we can get, due to the frequency resolution we are trying to achieve by selection of decomposition level. Consequently, the number of decomposition levels determine the smallest possible temporal window, in order to follow the temporal variations of RWE. In Table III, the minimum window sizes that can capture high-frequency components of each decomposition level are given. As the current signal is decomposed into 6 decomposition levels (as explained in Section V.A) in the proposed scheme, the minimum window size is selected as 1.28 ms.

The feature vectors are formulated by applying the time delays according to the selected embedding dimensions, as explained in Section IV.B. The extracted feature vector is then fed into ANN for fault classification. As discussed in Section IV, there are 2 feature vectors used for ANN training and fault classification in two relay types. The feature vectors X^I and X^{II} defined for two relays: *type I* (d = 2) and *type II* (d = 4) are represented by (4) and (5) respectively.

$$X^I = \begin{bmatrix} E_{1,t-1} & E_{1,t} \\ E_{2,t-1} & E_{2,t} \\ E_{3,t-1} & E_{3,t} \\ E_{4,t-1} & E_{4,t} \\ E_{5,t-1} & E_{5,t} \\ E_{6,t-1} & E_{6,t} \end{bmatrix} \qquad (4)$$

$$X^{II} = \begin{bmatrix} E_{1,t-3} & E_{1,t-2} & E_{1,t-1} & E_{1,t} \\ E_{2,t-3} & E_{2,t-2} & E_{2,t-1} & E_{2,t} \\ E_{3,t-3} & E_{3,t-2} & E_{3,t-1} & E_{3,t} \\ E_{4,t-3} & E_{4,t-2} & E_{4,t-1} & E_{4,t} \\ E_{5,t-3} & E_{5,t-2} & E_{5,t-1} & E_{5,t} \\ E_{6,t-3} & E_{6,t-2} & E_{6,t-1} & E_{6,t} \end{bmatrix} \qquad (5)$$

Where, $E_{1,t}$, $E_{2,t}$ …. $E_{6,t}$ are the RWE in the six decomposition levels of the t^{th} data window.

For clarity, only the feature vector X^{II}, i.e. RWE variation in the six decomposition levels within four temporal windows, under different fault and non-fault events are compared and discussed in this Section.

Different fault and non-fault cases were simulated under different configurations, and will be further discussed under Section VI.B. To identify a general trend, RWE variation for 25 randomly selected events (using PSCD/EMTDC simulated data) under different fault/ non-fault cases are shown in Fig. 4 and explained below:

a) ***DC side pole-ground fault***- RWE distribution of extracted feature vectors at the time of occurrence of pole-ground faults (set of 25 pole-ground fault events simulated under different fault configurations, such as with different fault resistances, locations, incident

This article has been accepted for publication in a future issue of this journal, but has not been fully edited. Content may change prior to final publication. Citation information: DOI 10.1109/ACCESS.2019.2945397, IEEE Access

times, etc.) is shown in Fig. 4(a). A general trend immerged shows that there is a sudden increase of RWE in decomposition level 2 in all the time steps, compared with the feature vectors during other non-fault events and pole-pole fault events. Since the set of 25 fault events under consideration in this figure represents a wide range of fault resistances and fault locations, it is clear that the trend of RWE distribution is typical to the pole-ground faults in DCMGs.

b) ***DC side pole–pole fault***- RWE distribution of feature vectors extracted at the time of occurrence of DC side pole-pole faults (set of 25 pole-pole fault events simulated under different fault configurations, such as with different fault resistances, locations, incident times, etc.) is shown in Fig. 4(b). The results clearly show an increase of RWE in decomposition levels 3 and 4 compared to pole-ground fault and other non-fault events. These characteristic variations are visible in all 25 pole-pole fault events considered in Fig. 4(b); hence, are typical to the pole-pole faults in DCMGs

c) ***Normal operation***- As can be seen from Fig. 4(c), the energy activity of a healthy network under normal operation (simulated for different modes of operation under different loading conditions) is different from that of a faulty network. Therefore, by comparison of feature vectors fault events can be differentiated from normal operation of the DCMG.

d) ***Load switching-***During the load switching operation of a healthy network (step changes of load by ±5%, ±10%, ±15%, ±20%, ±30%, ±40%) , there is an increase in energy levels in decomposition levels 5 and 6 (see Fig. 4(d)), compared with other fault and non-fault events. This characteristic RWE variation allows load switching operations to be distinguished from that of fault events.

e) ***Fault interruption in lateral feeders-*** Upon detection of a fault in a lateral feeder by primary protection relay of a lateral load feeder (relays R_4, R_5, R_6 and R_7), the fault zone of the network is isolated by the DC circuit breakers positioned at zones 2, 3, 4 and 5. The feature vectors are extracted from the current signal at the instance of pole-ground faults occurrence and immediate interruption (see Fig. 4(e)). The trend of RWE variation indicates the occurrence of pole-ground faults in first two data windows (***t-3*** and ***t-2***) as the RWE in decomposition level 2 is more dominant, similar to that of pole- ground faults (see Fig. 4(a)). However, the energy variation in the decomposition levels of the next two data windows (***t-1*** and ***t***) indicates that the fault is interrupted, and the RWE distribution differs from that of pole-ground fault. This characteristic temporal variation of RWE within 4 time windows indicates that a pole-ground fault has occurred and have been isolated. Hence, the event is classified as a fault event in the network, but does not require the relays R_1, R_2 and R_3 to operate as the faulted zone is already isolated.

Through the above analysis, it is clear that the capability of the proposed scheme to identify fault events can be realized by comparing the extracted feature vector. The extracted feature vector is then used as input of a feed-forward ANN for event classification, and is discussed under the next Section.

Intermediate stages of signal processing (at relay R_1) from simulated current waveforms up to ANN for fault detection and classification are presented in Fig. 5 for a fault (DC bus pole- ground fault) and non-fault (load switching operation) event. The comparison shows how each signal processing stage contributes in constructing the feature vector, which is then fed into the ANN model for classification.

VI. ARTIFICIAL NEURAL NETWORKS FOR FAULT DETECTION AND CLASSIFICATION

The proposed fault detection algorithm (see Fig.2) employs ANN to classify fault and non-fault events. ANN uses a soft criterion for feature comparison, and has the ability to infer the underlying nonlinear and complex relationships between input and output data [28, 39, 40]. In the process of training the ANN, the training algorithm is presented with sets of input data and output labels. Through iterative training procedure, the ANN weights and biases are adjusted by error signal in a way that the network output tries to follow the desired output [40-42].

A. NEURAL NETWORK STRUCTURE

The training parameters and structure of the two ANNs used in this study are shown in Table IV. They were selected to obtain the best classification performance, using a trial and error approach with different input feature vectors, the number of hidden layers, learning rates and activation functions. The selected structures of the two ANNs manifest the best classification accuracy. The ANN structure used for fault detection and classification in a *type II* relay is shown in Fig. 6. As discussed earlier, in a *type II* relay feature vector of 24 elements is employed to feed the ANN for event classification. Four output classes are defined for the four cases, i.e. normal operation, pole-ground fault, pole-pole fault and fault interruption operation in lateral feeders.

B. TRAINING/ TIME SERIES SIMULATION

The learning parameters of the ANN needs to be trained offline. To train the ANN with supervised learning algorithm, sufficient previous knowledge that represents fault and non-fault events under different operating conditions is a necessity. Furthermore, the training data should include adequate information to lead the tuning of the ANN parameters, approximating the system behavior [43, 44].

This article has been accepted for publication in a future issue of this journal, but has not been fully edited. Content may change prior to final publication. Citation information: DOI 10.1109/ACCESS.2019.2945397, IEEE Access

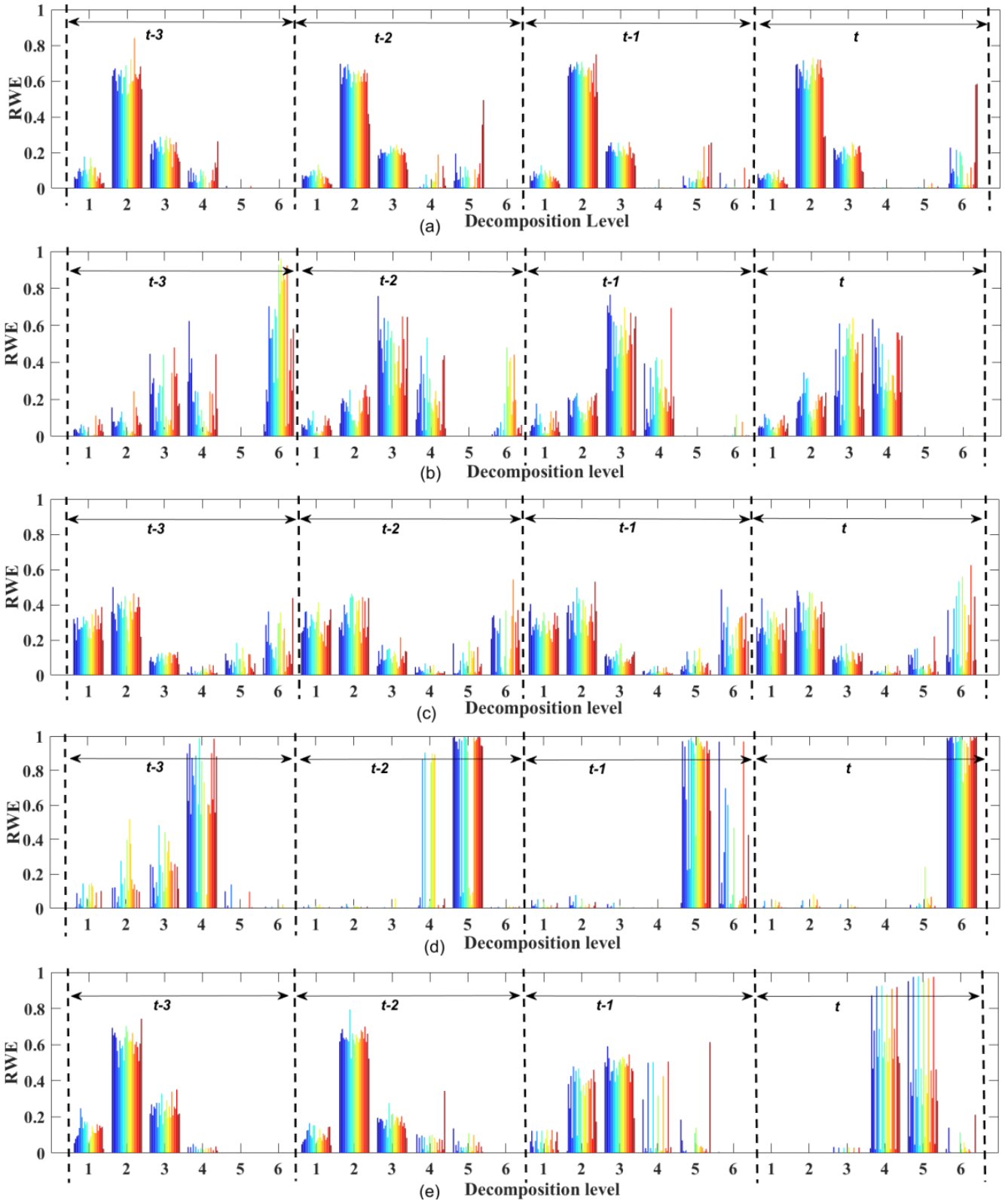

FIGURE 4: **RWE distribution diagram of the feature vector extracted from a) current signals during 25 pole- ground faults b) current signals during 25 pole-pole faults c) current signals during 25 normal operation conditions d) current signals during 25 load switch in-out operations e) current signals during 25 fault interruption operations by the primary protection relay of a lateral feeder.**

This article has been accepted for publication in a future issue of this journal, but has not been fully edited. Content may change prior to final publication. Citation information: DOI 10.1109/ACCESS.2019.2945397, IEEE Access

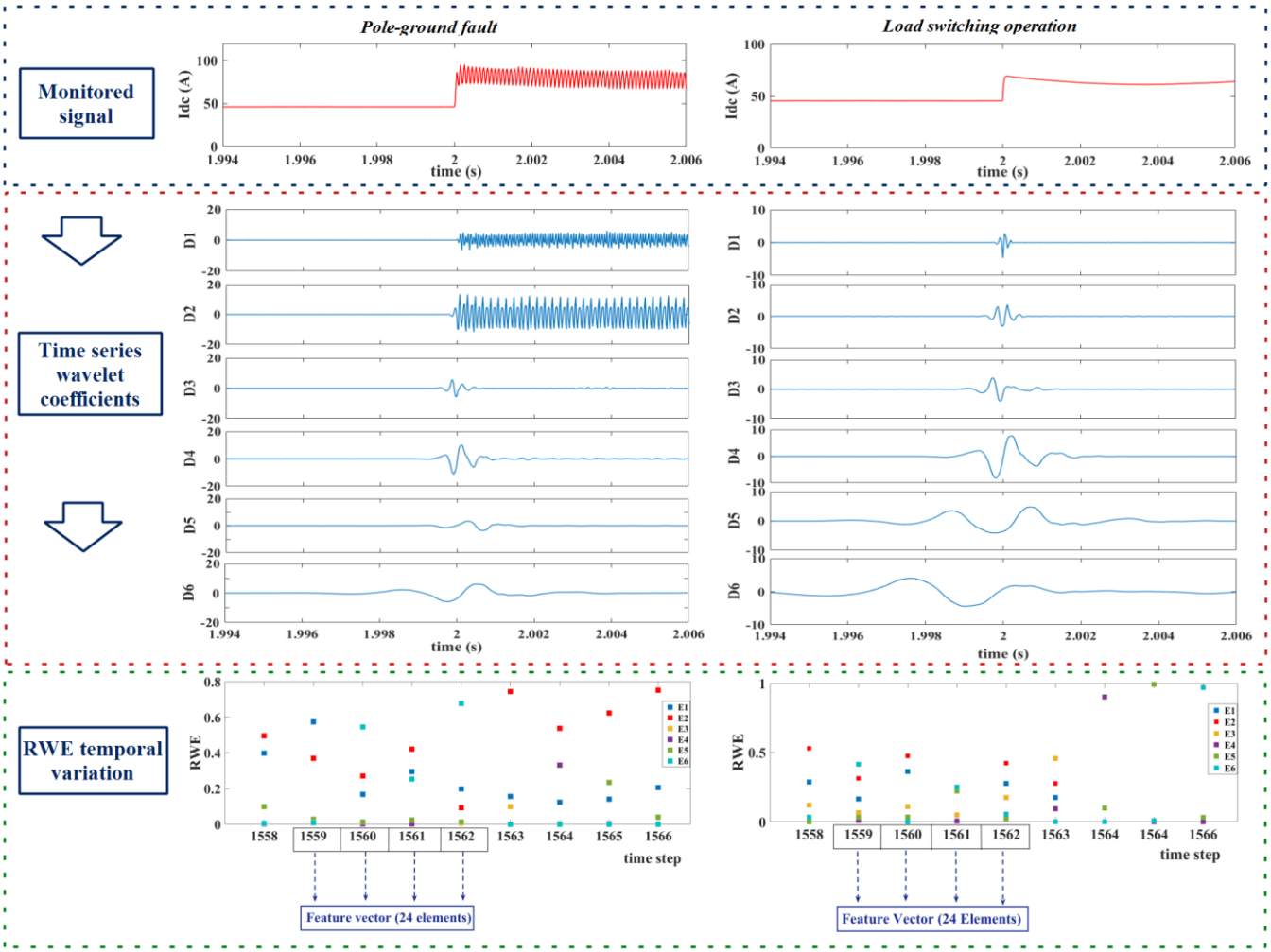

FIGURE 5: **Intermediate stages of signal processing for current signals with pole-ground fault (at t=2s), and load switching operation (at t=2s)**

The training data composed of both fault and non-fault current measurements can be either obtained from historical data or time-series simulations. In this study, training data is generated using the DCMG model (see Fig. 1) discussed in Section II, using PSCAD/EMTDC time-series simulations. Fault simulations with different fault types, fault resistances, fault locations under different loading levels and operating modes were carried out. In addition, non-fault cases including dynamic events such as load switching, operating mode changes were simulated under different conditions and are presented in Table V. In total, 1800 fault events and 3400 non-fault events are simulated for ANN training and testing.

The simulated data is divided into two, for training and testing by the ratio 3:1. The training data set is employed to train the learning parameters of the ANN, and testing data set to assess the classification accuracy of the developed machine learning model. Furthermore, by employing test data for validation, over-fitting problem (ANN model learning from noise and random variations in the training data, resulting in poor generalization performance over new data) can be avoided.

TABLE IV
ANN ARCHITECTURE AND LEARNING PARAMETERS FOR RELAY TYPE I AND II

ANN architecture and learning parameter	***Relay type I***	***Relay type II***
Number of layers	3	3
Number of Neurons	Input layer:24 Hidden layer:20 Output layer:4	Input layer:12 Hidden layer:10 Output layer:3
Activation function	Tangent sigmoid	Tangent sigmoid
Learning rule	Levenberg–Marquardt Back-Propagation	Levenberg–Marquardt Back-Propagation
Mean squared error	$1x\ 10^{-5}$	$1x\ 10^{-5}$

This article has been accepted for publication in a future issue of this journal, but has not been fully edited. Content may change prior to final publication. Citation information: DOI 10.1109/ACCESS.2019.2945397, IEEE Access

TABLE V
CONFIGURATIONS FOR FAULT AND NON FAULT SIMULATION IN PSCAD/EMTDC

Variable parameter	Configurations
Fault type	DC Pole- ground, DC Pole-pole (includes DC arc faults)
Fault resistance	0.01Ω- 300Ω
Fault location	DC bus, load feeders 1, 2, 3 and 4
Operating mode	Grid-connected, Islanded
Load feeders (zone 2, 3, 4 and 5) –loading level	Load feeder of zone 2: 20kW – 0kW Load feeder of zone 3: 20kW- 0kW Load feeder of zone 4: 20kW-0kW Load feeder of zone 5: 20kW- 0kW
Load switching	Load feeder step changes by ±5%, ±10%, ±15%, ±20%, ±30%, ±40%
Fault interruption operation in lateral feeders	Faults isolated by the lateral feeder primary protection relays R_4, R_5, R_6 and R_7 due to; pole- ground faults and pole-pole faults.

VII. PERFORMANCE TESTING AND DISCUSSION

To evaluate the fault detection and localization performance of the proposed scheme, the classification accuracies are calculated for each relay R_1-R_7, using the test data extracted from simulations. Table VI presents the sensitivity (how good at detecting the event) and precision (how many classified events are correctly classified) of each relay in detecting the network events, and overall classification accuracy. From Table VI, each relay has achieved more than 98% overall classification accuracy. The test results show that the developed protection scheme performs successfully in most test cases.

To provide better visualization of the performance of the developed scheme, the confusion matrix of the relay R_1 for test cases is shown in Fig. 7. In the figure, the output classes 1, 2, 3 and 4 represent the cases: normal operation, pole-ground fault, pole-pole fault and fault interruption operation in lateral feeders, respectively. The diagonal cells show the events that were correctly classified, while off-diagonal cells show the misclassified events. Target class represents the true event while the output class represents the predicted event from the classifier. We can see that pole-ground fault is misclassified as a normal operational event, while fault interruption operation is classified as a ground fault in zone 1 of the network (zone of the network protected by relay R_1).

The proposed scheme is capable of producing fault information in a very short duration as:

- Relays: *type I*- in less than 3 ms [Embedding time delay (=2.56 ms) + computational time (<100 µs)]
- Relays: *type II*- in less than 5.5 ms [Embedding time delay (=5.12 ms) + computational time (<100 µs)]

Temporal data embedding time delay constitutes a major part of fault detection time. For *type I* relay, embedding time delay can be calculated as; ($\boldsymbol{d}$=2) × (temporal window size= 1.28 ms) = 2.56 ms. Similarly, for a *type II* relay, embedding time delay is calculated as; ($\boldsymbol{d}$=4) × (temporal window size= 1.28 ms) = 5.12 ms. Considering the relatively low computational complexity of DWT Mallat algorithm [34] and ANN structure, computational time of the proposed algorithm was calculated to be less than 100 µs, assuming all calculations to be sequential. Hence, it can be concluded that the proposed scheme is very fast in terms of computational time, and thus supports online implementation.

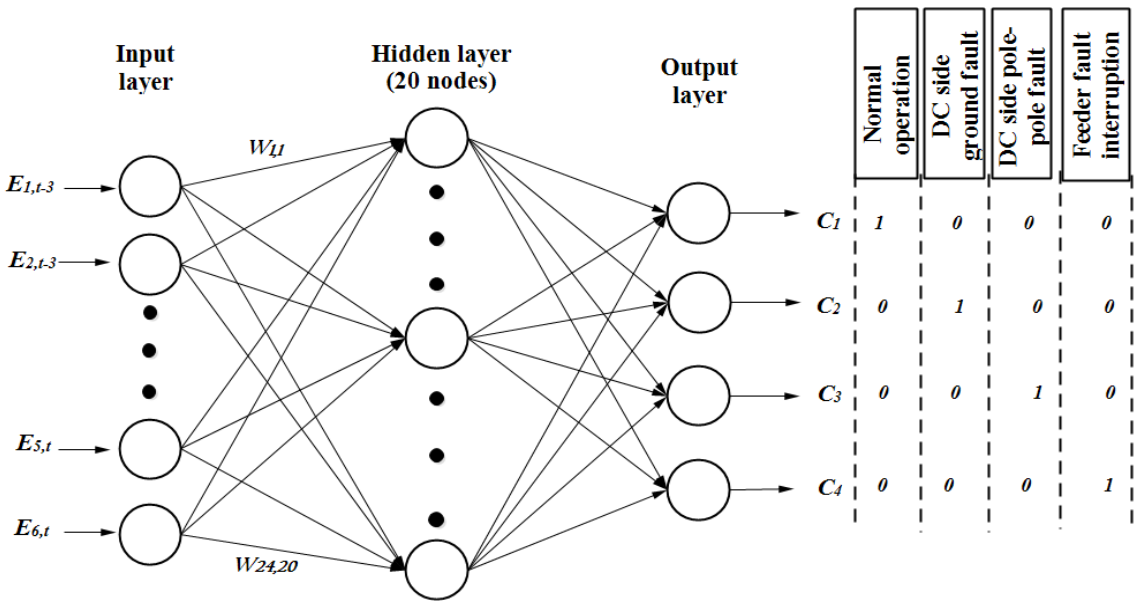

FIGURE 6: ANN structure for fault detection and classification in a *type II* relay.

This article has been accepted for publication in a future issue of this journal, but has not been fully edited. Content may change prior to final publication. Citation information: DOI 10.1109/ACCESS.2019.2945397, IEEE Access

TABLE VI
CLASSIFICATION ACCURACIES OF THE DEVELOPED FAULT DETECTION SCHEME

Relay (*type*)	No of test data sets	Sensitivity				Precision				Overall classification accuracy
		Normal operation	Pole-Ground fault	Pole-pole fault	Fault interruption operation	Normal operation	Pole-Ground fault	Pole-pole fault	Fault interruption operation	
R1 *(type II)*	200	100%	96.2%	100%	97.7%	99.0%	96.2%	100%	100%	**99.0%**
R2 *(type II)*	180	98.8%	100%	96.8%	97.6%	98.8%	100%	93.8%	100%	**98.3%**
R3 *(type II)*	200	99.0%	100%	100%	97.7%	99%	96.3%	100%	100%	**99.0%**
R4 *(type I)*	180	99.1%	100%	97.4%	-	99.1%	100%	97.4%	-	**98.9%**
R5 *(type I)*	180	100%	97.3%	100%	-	99.1%	100%	100%	-	**99.4%**
R6 *(type I)*	180	99.1%	97.3%	100%	-	99.1%	100%	97.4%	-	**98.9%**
R7 *(type I)*	180	99.1%	100%	94.7%	-	98.2%	100%	97.3%	-	**98.3%**

DC breakers technologies capable of meeting strict time and current limits imposed on DC networks is a vital requirement for DC network protection. There are several solid-state circuit breakers models and hybrid circuit breakers models for DC fault current interruption. Solid-state circuit breakers have typical breaker operating times of less than 100 µs, while hybrid circuit breakers are capable of operating in less than 1 ms [8-10]. These fast-acting DC circuit breaker models can be incorporated at each relay locations (at R_1 – R_7 in Fig. 1). Thus, it allows faults to be interrupted quickly once they are detected by the proposed scheme.

A. ROBUSTNESS OF THE PROPOSED SCHEME

To investigate the robustness of the proposed schemes to the impact of noisy branch current measurements, current time-series signals are added with white Gaussian noise. The feature vectors are extracted from these signals to formulate the test data set. Typical signal to noise ratio (SNR) values of 40 dB, 30 dB and 20 dB are used, and performance of the relay R_1 with test cases are summarized in Table VII.

TABLE VII
COMPARISON OF THE CLASSIFICATION ACCURACY OF RELAY I WITH ADDED NOISE TO THE CURRENT MEASUREMENTS

SNR	Overall classification accuracy
Without noise	99.0%
40 dB	98.5%
30 dB	98.0%
20 dB	97.0%

From the results, it can be seen that the noise in measurements only has an insignificant impact on the overall classification accuracy of the proposed scheme. In the considered worst case, SNR of 20 dB, overall classification accuracy decrease by only 2% compared to the results with current measurements without noise. Hence, it can be concluded that the signal noise only has a trivial impact on the performance of the proposed scheme.

B. COMPARISON WITH OTHER DCMG FAULT DETECTION SCHEMES.

Summary of comparison of the performance of the proposed scheme with the other DCMG fault detection schemes is provided in Table VIII. It can be concluded that the proposed technique is more effective in terms of detection accuracy, robustness to noise and smart fault detection capability.

Furthermore, the proposed scheme can successfully localize the fault to isolate the faulted zone quickly, without relying on communication and multi-terminal measurements, which was unavailable in the compared schemes.

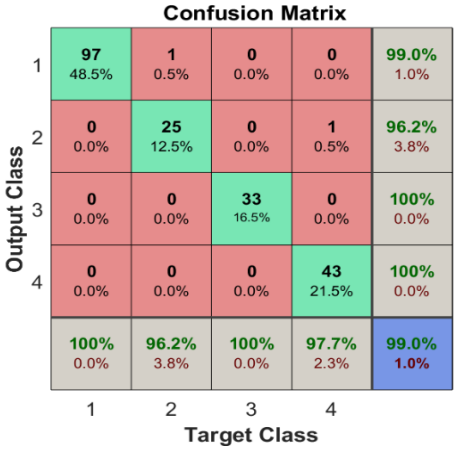

FIGURE 7: **Confusion matrix for event classification of relay R_1 with test data**

This article has been accepted for publication in a future issue of this journal, but has not been fully edited. Content may change prior to final publication. Citation information: DOI 10.1109/ACCESS.2019.2945397, IEEE Access

TABLE VIII
FAULT DETECTION SCHEMES FOR DC MICROGRIDS

Scheme	Fault localization and isolation capability	Communication requirements	Robustness to measurement uncertainty	Other remarks
Proposed scheme	Yes	No	Yes	• Overall fault classification accuracy of 98%-99%. • Intelligent fault detection capability with no communication. • Very fast selective fault isolation capability
Overcurrent+ Rate of current rise+ change of voltage [4]	No	No	No	• Less sensitivity to high impedance ground faults • Issues may arise in protection coordination
Overcurrent magnitude + direction of current [45]	Yes	Yes	Not mentioned	• Use communication between digital relays to locate the fault and isolate the faulted zone of the network
Overcurrent+ differential [5]	Yes	Yes	Not mentioned	• Use communication between digital relays to locate the fault and isolate the faulted zone of the network
Differential [3]	Yes	Yes	Not mentioned	• Rely on communication between protective relays on both sides of the protected zone for fault detection. • Drawbacks such as inability to provide backup protection.
Wavelet transform [16]	Yes	Yes	Not mentioned	• WT is applied to decompose common mode current at different network points to detect and locate ground faults
ANN [24, 25]	Yes	No	Not mentioned	• Directly use sampled current measurements for classification • Uses two neural networks for detection and location. • Fault location can be detected with a 1% error • Complex classifier structure, hence leading to long training and detection times.

VIII. CONCLUSION

This paper proposes a novel intelligent fault detection and localization scheme for DC microgrids, based on wavelet-multi resolution analysis and machine learning-based approach. The post-fault behavior of the network immediately indicates the occurrence of a fault. Current measurements can be used to extract features indicative of a fault event, using the wavelet transform as the signal processing tool. Different from previous work, use of ANN for classification of network events endows smartness to the scheme. It enables accurate fault detection unaffected by network operation mode, loading conditions, fault resistance, fault location, and other network events while being reliable even under noise in the measurements. Furthermore, this scheme can ensure quick identification of the fault location and isolation of the fault; hence, prevent damages to the network components caused by high fault currents and improves the network reliability. The proposing algorithm has very low computational burden due to fewer input data and computationally efficient nature of wavelet transform and ANNs, thus supports online implementation.

To ascertain the applicability of the proposed scheme with different DC network architectures requires further investigation. The analysis presented herein shows that the proposed scheme features reliable fault identification capability under various system changes. Hence, it stands to reason that the proposed fault detection and localization scheme can be generalized and applied to DC networks of different sizes and architectures.

APPENDIX

This Section briefly describes wavelet theory and its properties. Then we discuss the DWT based multi-resolution analysis, which serves the important task of feature extraction in the proposed scheme.

A. WAVELET THEORY

A family of wavelet, $\psi_{(a,b)}(t)$ is a set of elemental functions generated by scaling and translation of a unique admissible mother wavelet $\psi(t)$, and is given by (6),

$$\psi_{(a,b)}(t) = \frac{\psi}{\sqrt{a}}\left(\frac{t-b}{a}\right) \qquad (6)$$

Where, a and b are scaling and translation parameters, respectively.

This article has been accepted for publication in a future issue of this journal, but has not been fully edited. Content may change prior to final publication. Citation information: DOI 10.1109/ACCESS.2019.2945397, IEEE Access

Continuous wavelet transform (CWT) is defined as the correlation between the signal ***f(t)***, with the family wavelet $\Psi^*_{(a,b)}(t)$ for each ***a*** and ***b***, and defined as in (7) [10].

$$W_{(a,b)}(t) = \int_{\infty}^{-\infty} f(t)\, \psi^*_{(a,b)}(t)dt \qquad (7)$$

Here, $a, b \in \mathbb{R}$, $a \neq 0$ and * denotes the complex conjugate.

In principle, CWT provides a redundant representation of the signal under analysis. To overcome data redundancy and reduce calculation time, DWT has been introduced, where wavelets are scaled and translated into discrete steps [27, 28]. DWT is performed by discretizing ***a*** and ***b***. Typically, these parameters are set to powers of 2, so that sampling of the frequency axis corresponds to dyadic sampling and $\psi_{(j,k)}(t)$ is then given by (8),

$$\psi_{(j,k)}(t) = \frac{\psi}{\sqrt{2^j}}\left(\frac{t}{2^j} - k\right) \qquad (8)$$

and DWT is derived by (9),

$$d_{j,k} = \int_{\infty}^{-\infty} f(t)\, \psi^*_{(j,k)}(t)dt \qquad (9)$$

Where $d_{j,k}$ are the wavelet detail coefficients at decomposition level ***j*** and location ***k***.

B. MULTI RESOLUTION ANALYSIS

For most functions, ***f(t)***, wavelet transforms do not have an analytical solution, and they can only be solved by numerical approaches. Multi-resolution analysis framework for the representation of a signal at different scales is introduced in [27, 28]. Given a signal ***f(t)***, its multi-resolution decomposition at level ***M*** is defined by (10),

$$f(t) = \sum_k a_{M,k} \frac{\psi}{\sqrt{2^M}}\left(\frac{t}{2^M} - k\right) + \sum_k^M \sum_k d_{j,k} \frac{\psi}{\sqrt{2^j}}\left(\frac{t}{2^j} - k\right) \triangleq A_M(t) + \sum_j D_j(t) \qquad (10)$$

Where, $a_{M,k}$ are the approximation coefficients at level ***M***, and $\psi(t)$ is the scaling function. This transformation decompose the function ***f(t)*** into approximation coefficients, $A_M(t)$ and a series of detail coefficients, $D_j(t)$ [27, 28].

The DWT can be considered as a filter bank as shown in Fig. 8 where DWT is performed by passing the sampled signal ***x(n)*** through high pass filter, ***h(n)*** and a low pass filter, ***g(n)*** and output is decimated by 2 to compute both approximation coefficients, $A_M(t)$ and detail coefficients, $D_j(t)$. Here, $A_M(t)$ represents low-frequency components, while $D_j(t)$ represents high-frequency components. Assuming the signal sampling frequency to be ***f***, the c frequency bands corresponding to different decomposition levels are shown in Fig. 8.

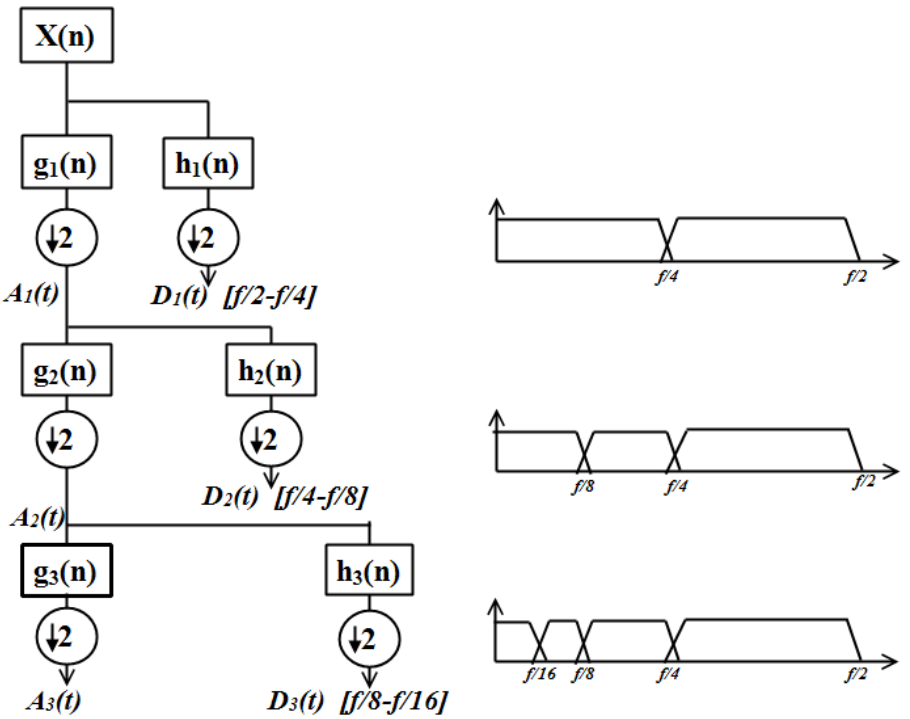

FIGURE 8: DWT decomposition of signal with iterated filter banks, and frequency bands of different decomposition levels

This article has been accepted for publication in a future issue of this journal, but has not been fully edited. Content may change prior to final publication. Citation information: DOI 10.1109/ACCESS.2019.2945397, IEEE Access

REFERENCES

[1] Salomonsson D, Sannino A. "Low-Voltage DC Distribution System for Commercial Power Systems with Sensitive Electronic Loads". *IEEE Transactions on Power Delivery* 2007;22:1620–7.

[2] Justo JJ, Mwasilu F, Lee J, Jung J-W. "AC-microgrids versus DC-microgrids with distributed energy resources: A review". *Renewable and Sustainable Energy Reviews* 2013;24:387–405.

[3] Fletcher S, Norman P, Galloway S, Burt G. "Optimizing the roles of unit and non-unit protection methods within DC microgrids". *2013 IEEE Power & Energy Society General Meeting* 2013.

[4] D. Salomonsson, L. Soder, and A. Sannino, "Protection of Low-Voltage DC Microgrids," *IEEE Transactions on Power Delivery*, vol. 24, no. 3, pp. 1045–1053, 2009.

[5] J.-D. Park, J. Candelaria, L. Ma, and K. Dunn, "DC Ring-Bus Microgrid Fault Protection and Identification of Fault Location," *IEEE Transactions on Power Delivery*, vol. 28, no. 4, pp. 2574–2584, 2013.

[6] Candelaria J, Park J-D. VSC-HVDC system protection: A review of current methods. 2011 IEEE/PES Power Systems Conference and Exposition 2011.

[7] Yang J, Fletcher JE, Oreilly J. "Short-Circuit and Ground Fault Analyses and Location in VSC-Based DC Network Cables". *IEEE Transactions on Industrial Electronics* 2012;59:3827–37

[8] Kempkes M, Roth I, Gaudreau M. "Solid-state circuit breakers for Medium Voltage DC power". *2011 IEEE Electric Ship Technologies Symposium* 2011

[9] Ryan DJ, Torresan HD, Bahrani B. "A Bidirectional Series Z-Source Circuit Breaker". *IEEE Transactions on Power Electronics* 2018;33:7609–21.

[10] Song X, Peng C, Huang AQ. "A Medium-Voltage Hybrid DC Circuit Breaker, Part I: Solid-State Main Breaker Based on 15 kV SiC Emitter Turn-OFF Thyristor". *IEEE Journal of Emerging and Selected Topics in Power Electronics* 2017;5:278–88.

[11] F. Ribeiro, *Power systems signal processing for smart grids*. Chichester, West Sussex: Wiley, 2014.

[12] N. W. A. Lidula and A. D. Rajapakse, "A Pattern-Recognition Approach for Detecting Power Islands Using Transient Signals—Part II: Performance Evaluation," in *IEEE Transactions on Power Delivery*, vol. 27, no. 3, pp. 1071-1080, July 2012.

[13] W. Li, M. Luo, A. Monti, and F. Ponci, "Wavelet based method for fault detection in Medium Voltage DC shipboard power systems," *2012 IEEE International Instrumentation and Measurement Technology Conference Proceedings*, 2012.

[14] K. Satpathi, Y. M. Yeap, A. Ukil, and N. Geddada, "Short-Time Fourier Transform Based Transient Analysis of VSC Interfaced Point-to-Point DC System," *IEEE Transactions on Industrial Electronics*, vol. 65, no. 5, pp. 4080–4091, 2018.

[15]S. Som and S. R. Samantaray, "Wavelet based fast fault detection in LVDC micro-grid," *2017 7th International Conference on Power Systems (ICPS)*, 2017.

[16] Yang R, Cuzner RM. "Single ground fault location algorithm in DC microgrid based on wavelet transform" . *2016 IEEE International Conference on Renewable Energy Research and Applications*, 2016.

[17] D. P. Mishra, S. R. Samantaray, and G. Joos, "A Combined Wavelet and Data-Mining Based Intelligent Protection Scheme for Microgrid," *IEEE Transactions on Smart Grid*, vol. 7, no. 5, pp. 2295–2304, 2016.

[18] W. Li, A. Monti, and F. Ponci, "Fault Detection and Classification in Medium Voltage DC Shipboard Power Systems with Wavelets and Artificial Neural Networks," *IEEE Transactions on Instrumentation and Measurement*, vol. 63, no. 11, pp. 2651–2665, 2014.

[19] J. J. Q. Yu, Y. Hou, A. Y. S. Lam, and V. O. K. Li, "Intelligent Fault Detection Scheme for Microgrids With Wavelet-Based Deep Neural Networks," *IEEE Transactions on Smart Grid*, vol. 10, no. 2, pp. 1694–1703, 2019.

[20] S. Kar, S. R. Samantaray, and M. D. Zadeh, "Data-Mining Model Based Intelligent Differential Microgrid Protection Scheme," *IEEE Systems Journal*, vol. 11, no. 2, pp. 1161–1169, 2017.

[21] E. Casagrande, W. L. Woon, H. H. Zeineldin, and N. H. Kan'an, "Data mining approach to fault detection for isolated inverter-based microgrids," *IET Gener. Transm. Distrib.*, vol. 7, no. 7, pp. 745–754, Jul. 2013.

[22] N. Perera and A. Rajapakse, "Recognition of fault transients using a probabilistic neural-network classifier," *2011 IEEE Power and Energy Society General Meeting*, Detroit, MI, USA, 2011, pp. 1-1.

[23] Mair A, Davidson E, Mcarthur S, Srivastava S, Schoder K, Cartes D. "Machine learning techniques for diagnosing and locating faults through the automated monitoring of power electronic components in shipboard power systems". *2009 IEEE Electric Ship Technologies Symposium,* 2009.

[24] Almutairy, I., & Alluhaidan, M. (2017). "Fault Diagnosis Based Approach to Protecting DC Microgrid Using Machine Learning Technique". *Procedia Computer Science*, 114, 449-456.

[25] Yang, Q., Li, J., Blond, S. L., & Wang, C. (2016). "Artificial Neural Network Based Fault Detection and Fault Location in the DC Microgrid". *Energy Procedia*, 103, 129-134

[26] D. K. J. S. Jayamaha, N. W. A. Lidula and A. D. Rajapakse, "Bus Voltage Signaling Based Coordinated Control of DC Microgrids," *2018 Australasian Universities Power Engineering Conference (AUPEC)*, Auckland, New Zealand, 2018, pp. 1-6..

[27] P. M. Anderson, *Power system protection*. New York: McGraw-Hill, 1999.

[28] M. A. Nielsen, *Neural Networks and Deep Learning*. Determination Press, 2015.

[29] M. Vafaeipour et.al "Application of sliding window technique for prediction of wind velocity time series," *International Journal of Energy and Environmental Engineering*, vol. 5, no. 2-3, 2014.

[30] R.J Frank., N. Davey & S.P. Hunt, "Time Series Prediction and Neural Networks", *Journal of Intelligent and Robotic Systems*, vol. 31, issue. 1-3, pp. 91-103, 2001.

[31] F. R. Gomez, A. D. Rajapakse, U. D. Annakkage and I. T. Fernando, "Support Vector Machine-Based Algorithm for Post-Fault Transient Stability Status Prediction Using Synchronized Measurements," in *IEEE Transactions on Power Systems*, vol. 26, no. 3, pp. 1474-1483, Aug. 2011.

[32] S. Chen and H. Y. Zhu, "Wavelet Transform for Processing Power Quality Disturbances," *EURASIP Journal on Advances in Signal Processing*, vol. 2007, no. 1, 2007.

[33] S. Avdakovic, A. Nuhanovic, M. Kusljugic, and M. Music, "Wavelet transform applications in power system dynamics," *Electric Power Systems Research*, vol. 83, no. 1, pp. 237–245, 2012.

[34] S. G. Mallat and Peyré Gabriel, *A wavelet tour of signal processing: the Sparse way*. Amsterdam: Elsevier /Academic Press, 2009.

[35] S. Mallat, "A theory for multiresolution signal decomposition: the wavelet representation," *IEEE Transactions on Pattern Analysis and Machine Intelligence*, vol. 11, no. 7, pp. 674–693, 1989.

[36] W. K. Ngui, M. S. Leong, L. M. Hee, and A. M. Abdelrhman, "Wavelet Analysis: Mother Wavelet Selection Methods," *Applied Mechanics and Materials*, vol. 393, pp. 953–958, 2013.

[37] O. Rosso, M. Martin, A. Figliola, K. Keller, and A. Plastino, "EEG analysis using wavelet-based information tools," *Journal of Neuroscience Methods*, vol. 153, no. 2, pp. 163–182, 2006.

[38] L. Guo, D. Rivero, J. A. Seoane, and A. Pazos, "Classification of EEG signals using relative wavelet energy and artificial neural networks," *Proceedings of the first ACM/SIGEVO Summit on Genetic and Evolutionary Computation - GEC 09*, 2009.

This article has been accepted for publication in a future issue of this journal, but has not been fully edited. Content may change prior to final publication. Citation information: DOI 10.1109/ACCESS.2019.2945397, IEEE Access

[39] Ç. Kocaman and M. Özdemir, "Comparison of statistical methods and wavelet energy coefficients for determining two common PQ disturbances: Sag and swell," *2009 International Conference on Electrical and Electronics Engineering -, Bursa*, 2009, pp. I-80-I-84.

[40] R. Lippmann, "An introduction to computing with neural nets," *IEEE ASSP Magazine*, vol. 4, no. 2, pp. 4–22, 1987.

[41] S. Chen and S. A. Billings, "Neural networks for nonlinear dynamic system modelling and identification," *International Journal of Control*, vol. 56, no. 2, pp. 319–346, 1992.

[42] "What Is a Neural Network?," - MATLAB & Simulink. [Online]. Available: https://www.mathworks.com/discovery/neural-network.html.

[43] N. K. Chanda and Y. Fu, "ANN-based fault classification and location in MVDC shipboard power systems," *2011 North American Power Symposium*, 2011.

[44] Q. Yang, S. L. Blond, R. Aggarwal, Y. Wang, and J. Li, "New ANN method for multi-terminal HVDC protection relaying*," Electric Power Systems Research*, vol. 148, pp. 192–201, 2017.

[45] Emhemed AAS, Burt GM. "An Advanced Protection Scheme for Enabling an LVDC Last Mile Distribution Network". *IEEE Transactions on Smart Grid* 2014;5:2602–9.

D.K.J.S Jayamaha received his B.Sc. (Eng). degree from University of Moratuwa, Sri Lanka, in 2017. Currently he is reading for his MPhil degree at the Department of Electrical Engineering, University of Moratuwa. His research interests include microgrids, distributed and renewable energy systems and power system protection.

N. W. A. Lidula (GS'09–M'12) received her B.Sc. (Eng.) degree and M.Sc. degree from the University of Moratuwa, Sri Lanka, in 2002, and 2004 respectively. She received the M.Eng. degree from the Asian Institute of Technology, Bangkok, Thailand, in 2006, and the Ph.D. degree in Electrical and Computer Engineering from the University of Manitoba, Winnipeg, MB, Canada in 2012. Currently she is a Senior Lecturer at the University of Moratuwa, Sri Lanka. Her research interests include microgrids, distributed generation, power system stability, transient simulation of power systems and renewable energy systems. ORCid: https://orcid.org/0000-0003-3556-4693

Athula D. Rajapakse (M'99–SM'08) received the B.Sc (Eng.) degree in electrical engineering from the University of Moratuwa, Katubedda, Sri Lanka, in 1990, the M. Eng. degree in energy (Energy Technology) from the Asian Institute of Technology, Bangkok, Thailand, in 1993, and the Ph.D degree in quantum engineering and systems science from the University of Tokyo, Tokyo, Japan, in 1998.,He is currently a Professor with the University of Manitoba, Winnipeg, MB, Canada. He is a Registered Professional Engineer in the province of Manitoba, Canada. His research interests include power system protection, grid integration of distributed and renewable energy systems, and protection of future DC grids.